Advanced Bends and Micro Ring Resonators in Silicon Nitride Photonic Waveguides for C-Band

Jeong Hwan Song, Tangla D. Kongnyuy, Mathias Prost, Aritrio Bandyopadhyay, Sarvagya Dwivedi, *Member, IEEE*, Diego Carbajal Altamirano, Cian Cummins, Sandeep Seema Saseendran, Philippe Helin, Joost Brouckaert, and Marcus Dahlem, *Senior Member, IEEE*

***Abstract*—We present the design and experimental evaluation of low-loss advanced bends in silicon nitride (SiN) waveguides for the C-band. The advanced bends, with a radius of 25 μm, exhibit a bending loss of approximately 0.025 dB per 90°, comparable to the loss of a circular bend with a radius of 50 μm. Consequently, the 25 μm radius advanced bend is proposed for routing in SiN photonic integrated circuits to reduce the overall footprint. Furthermore, the use of these advanced bends in micro ring resonators results in quality factors of 5.8×10^3 and 5.5×10^4, with relatively large free spectral ranges and extinction ratios for radii of 15 μm and 25 μm, respectively.**

***Index Terms*—Bends, integrated optics, ring resonators, silicon, silicon nitride, silicon nitride bends, silicon nitride waveguide, silicon photonics, waveguides.**

I. Introduction

SILICON Nitride (SiN) waveguides are transparent over a wide range of wavelengths, making them suitable for various applications, including visible and infrared light for life science sensors, as well as O-, C-, and L-bands for data and telecommunication systems. SiN waveguides are particularly competitive with silicon (Si) waveguides for O-, C-, and L-band applications due to several advantages. Compared to Si waveguides, SiN-based photonic circuits exhibit lower nonlinearity, lower propagation loss, and greater thermal stability. However, SiN-based photonic circuits have larger footprints compared to Si-based circuits due to the relatively low index contrast. The footprints of photonic circuits are mainly dependent on the critical radii of the bending waveguides. Typically, photonic circuits with Si and SiN waveguides use minimum radii of 5 μm and 50 μm, respectively. However, bends with these radii still incur losses.

Efforts are ongoing to minimize the existing bending losses of critical bending radii and to achieve smaller critical radii for SiN photonic waveguides. For example, one classical approach involves implementing an offset between bent and straight waveguides [1], while another method uses special bends [2], [3], [4], [5], [6], [7], [8]. In 2019, we proposed advanced bends using waveguide widening with sinusoidally varying radii. These advanced bends were experimentally demonstrated on Si waveguides for the C-band and SiN waveguides for the infrared wavelength of 850 nm [3], [4]. We believe that studying the reduction of bend loss and radius for SiN bending waveguides is of greater importance than for Si bending waveguides. Despite the significance of this topic, there are few experimental results in the literature regarding smaller radius SiN bending for the C-band. Table I summarizes the experimental results of SiN waveguide bends as reported in major journals [4], [5], [6], [7], [8].

In this paper, we present the designs of the advanced bends for the C-band along with measurement results of fabricated structures on the SiN waveguide platform using IMEC's pilot line. We conducted measurements and analysis on the fabricated SiN bends and present the results of micro ring resonators that incorporated these advanced bends.

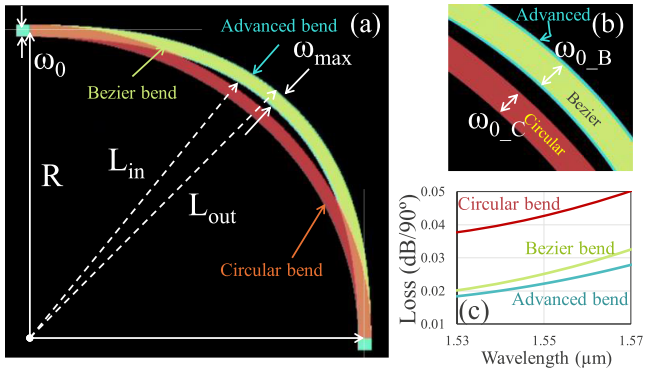

Fig. 1. (a) Advanced bend configuration and its design parameters. (b) Zoom in at near 45 degree angle with bending profile comparison of our work, a Bezier and circular bends (ω_{max} is wider than ω_{0_B}.). (c) Bending loss comprison. Here, ω_{0_C} and ω_{0_B} are widths of a circular and a Bezier bends, respectively.

II. Advanced Bends for SiN Waveguides

The design of the advanced bends is described by following [4]. Fig. 1(a) shows the definition of parameters.

$$L_{out}(n) = R + \frac{1}{2}\left(\omega(n) + \frac{1}{k_1}\sin(4\theta_n)\right) \quad (1)$$

Received 11 November 2024; revised 25 November 2024; accepted 26 November 2024. Date of publication 29 November 2024; date of current version 12 December 2024. This work was supported by Horizon 2020 Framework Programme under Grant 101017088 (INSPIRE). *(Corresponding author: Jeong Hwan Song.)*

Jeong Hwan Song, Tangla D. Kongnyuy, Mathias Prost, Aritrio Bandyopadhyay, Diego Carbajal Altamirano, Cian Cummins, Sandeep Seema Saseendran, Philippe Helin, Joost Brouckaert, and Marcus Dahlem are with IMEC, 3001 Leuven, Belgium (e-mail: jeonghwan.song@imec.be).

Sarvagya Dwivedi was with IMEC, 3001 Leuven, Belgium. He is now with Texas Instruments Inc, Dallas, TX 75243 USA.

Digital Object Identifier 10.1109/JPHOT.2024.3509312

© 2024 The Authors. This work is licensed under a Creative Commons Attribution 4.0 License. For more information, see https://creativecommons.org/licenses/by/4.0/

TABLE I
REVIEW OF EXPERIMENTAL RESULTS OF SMALL RADIUS SiN BANDS SHOWN IN PUBLICATIONS

Reference# / year	Effective R	Bending loss	Wavelength	Single mode waveguide (W × H)	Method	Process	Propagation loss
[4] / 2020	5μm	1.82dB/90°	850nm	600nm × 300nm	Widening and sinusoidally varying radii (advanced)	PECVD	0.3dB/cm
	10μm	0.25dB/90°					
	15μm	0.04dB/90°					
	20μm	0.01dB/90°					
[5] / 2016	3μm	1.403dB/90°	638nm	450nm × 220nm	Widening with offset circular radii	PECVD	1.0dB/cm
	4μm	0.633dB/90°					
	5μm	0.215dB/90°					
	7μm	0.054dB/90°					
	10μm	0.034dB/90°					
[6] / 2021	30μm	0.037dB/90°	1550nm	1000nm × 400nm	Euler spiral based	PECVD SiN on SOI	NA
	40μm	0.031dB/90°					
	50μm	0.023dB/90°					
[7] / 2022	8μm	1.225B/90°	1550nm	1200nm × 400nm	Modified Bezier bend (widening with Bezier)	LPCVD	NA
	10μm	0.525dB/90°					
	12μm	0.32dB/90°					
[8] / 2019	50μm	0.008dB/90°	850nm	680nm × 160nm	Partial Euler bend	NA	NA

$$L_{in}(n) = R - \frac{1}{2}\left(\omega(n) + \frac{1}{k_2}\sin(4\theta_n)\right) \quad (2)$$

$$\omega(n) = \omega_{n-1} + \frac{1}{2}\left(\frac{1}{k_1} + \frac{1}{k_2}\right)\sin(4\theta_n), \omega_0 = C \quad (3)$$

Here, R represents the minimum distance between point (0, 0) and the center of the bending waveguide (intuitively, the value corresponds to the radius of a circular bend.), and θ and n correspond to the angle of bends and the order of segments, respectively. For example, $\Delta\theta = 1°$ and n = 1, 2, 3, …, 90 (integer) for 90° bends. $\theta_n = n \times \Delta\theta$. k_1 and k_2 represent bending coefficients. Optimized values of k_1 and k_2 were determined through 3-dimensional Finite-Difference Time-Domain (3D-FDTD) simulations. $\omega(n)$ refers to the varying width of the waveguide by segments and $\omega_0 = C\ (constant)$. Here, $C = 1\ \mu$m as the initial waveguide width when n = 1. Finally, the bend shape is described by following equation: $(x, y) = (L(n)\cos(\theta_n), L(n)\sin(\theta_n))$. These equations can be universally used for designing bend shapes. When k_1 and k_2 approach infinity, the radius becomes constant, resulting in a normal circular bend.

We compared between the advanced bend and Bezier bend as shown in Fig. 1(a) and (b). The cubic Bezier curve is expressed as $P(t) = (1-t)^3 P_0 + 3(1-t)^2 t P_2 + 3(1-t)t^2 P_3 + t^3 P_1$ where the curve parameter (t) varies from 0 to 1. The curve is defined by four coordinates $P(t) = (x(t), y(t))$. P_0 at $(0, 0)$ and P_1 at (R, R) are the starting and ending points, respectively. The middle two points, P_2 of $(R(1-B), 0)$ and P_3 of (R, RB), are optimized by B $(0 < B < 1)$.

Fig. 1(b) magnifies the bending profiles of the Bezier and our method. The bending profile of the advanced bend resembles a cubic Bezier curve when the Bezier coefficient (B) is 0.32. In this case, the maximum distance (L_{max}) between the center of the waveguide and the center of curvature at 45 degrees, which is the smallest radius of curvature, of a 90-degree bend matches the advanced bend. The matched L_{max} is 26.69 μm. A smaller B is expected to have smaller bending losses than the circular bend (*c.f.* $B = 0.45$, equivalent to the circular bend [9]). Fig. 1(c) shows the simulation results of three bends when $R = 25\ \mu$m. Here, the widths of the waveguides, ω_0, ω_{0_B}, and ω_{0_C}, are all 1 μm. The key difference in our approach is the widening of the bending waveguides, even though the bending profile remains similar. Wider waveguides have a higher effective index and confinement factor, which can result in smaller critical bending radii.

Another method is the Euler bend. The curvature of the Euler bend increases linearly [6] (*c.f.* the curvature of a circular bend is constant), leading to rapid curvature variation at the center and a quick reduction in bending radius, resulting in high radiation losses. Therefore, a partial Euler bend was introduced to reduce high radiation losses in the center of the bend [8].

An interface between straight and bending waveguides can cause losses due to the misalignment of their propagation axes.

TABLE II
SIMULATION RESULTS OF ADVANCED AND CIRCULAR BENDS WITH PARAMETERS

Radius (R) / effective [μm]	Advanced bends			Circular bends		
	15	20	25	15	20	25
ω_0 [μm]	1	1	1	1	1	1
ω_{max} [μm]	1.25	1.5	1.2	1	1	1
k_1	15	10	8	Inf.	Inf.	Inf.
k_2	-20	-15	-9	Inf.	Inf.	Inf.
Bending loss at 1550nm [dB/90°]	0.087	0.027	0.022	0.134	0.066	0.048

Therefore, special bends, such as Advanced (our method), Bezier, and Euler bends, minimize this loss by gradually changing and optimizing curvature radii. Intentional offsets can also be implemented [1], [5].

Width-widening Bezier bends, recently proposed as modified Bezier bends, were introduced [7]. The approach of modified Bezier bends requires the optimization of four coefficients to find the optimal bend. However, our approach only requires two coefficients, making it more efficient. The experimental data from the literature [4], [7] clearly showed different results. For example, for an advanced bend and modified Bezier bend with a radius of 2 μm in Si waveguides, the experimental bending losses were 0.012 dB/90° [4] and 0.028 dB/90° [7] from our design (advanced bend) and the modified Bezier bend, respectively. For further comparison, circular bends with a radius of 2 μm had losses of 0.079 dB/90° [4] and 0.066 dB/90° [7].

The SiN waveguide platform has the following parameters: the refractive indexes of the SiN core and the oxide cladding are approximately 2.0 and 1.44, respectively. For single-mode operation, the chosen width and thickness of the core are 1000 nm and 400 nm, respectively at a wavelength of 1550 nm.

The advanced bends with radii of 15 μm, 20 μm, and 25 μm were optimized by 3D-FDTD simulations. The optimized bending coefficients, widening width, and simulation results with normal bends are summarized in Table II. The losses in circular bends are nearly twice as high as those in advanced bends. All simulations were implemented with a fundamental transverse electric (TE) mode.

III. EXPERIMENTAL RESULTS

The test structures with the bends were fabricated on IMEC's SiN technology platform using the Low-Pressure Chemical Vapor Deposition (LPCVD) process. The waveguide consists of a ~400 nm-thick silicon nitride layer with top and under cladding of ~2.0 μm and ~2.7 μm, respectively. The under-cladding thickness of 2.7 μm is sufficient to prevent substrate leakage during propagation. Additionally, this thickness is optimal for the directionality of grating couplers used for fiber coupling.

The platform's propagation losses for 1 μm-width waveguides range from 0.08 dB/cm to 0.4 dB/cm with a C-band light source [10]. These propagation losses vary from wafer to wafer due to differences in layer stacks. The pure propagation loss of a bend

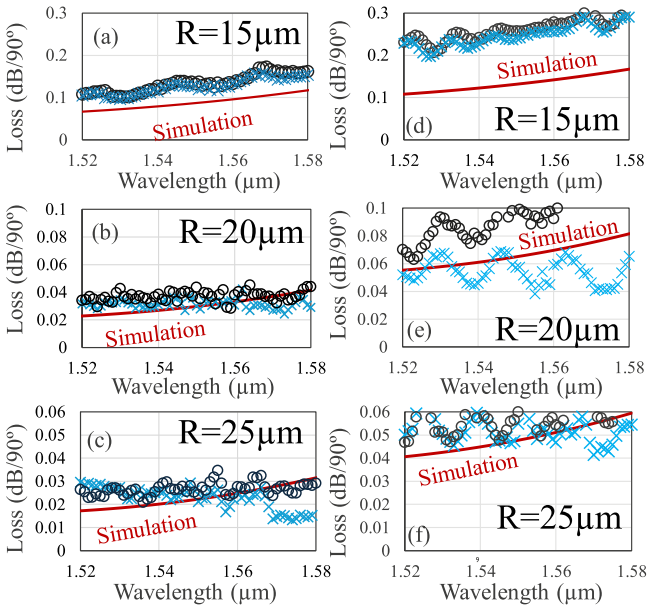

Fig. 2. Measurement results: (a)–(c) Advanced bends and (d)–(f) circular bends (solid line: 3D-FDTD, o and x: Measurement on different dies/wafers).

TABLE III
EXPERIMENTAL RESULTS OF ADVANCED AND CIRCULAR BENDS

Radius (R) / effective [μm]	Advanced bends			Circular bends		
	15	20	25	15	20	25
Bending loss at 1550nm [dB/90°]	0.13	0.03	0.025	0.25	0.08	0.055

with a 50 μm radius, excluding bending radiation loss, is 0.0006 dB/90° and 0.003 dB/90° when the propagation losses are 0.08 dB/cm and 0.4 dB/cm, respectively. A wider waveguide width results in lower propagation loss compared to the 1 μm-width waveguide. For a 2.5 μm-width waveguide, we measured propagation losses of less than 0.05 dB/cm. Therefore, the advanced bend benefits from reduced pure propagation loss due to the increased width.

Fig. 2 shows the measurement results of advanced bends and circular bends for comparison. As anticipated, advanced bends exhibit significantly lower bending losses compared to circular bends. Each measurement point is derived from a linear fit to the data set of four different numbers of bends, providing estimated bend losses across the full range of the C-band. The measurement was implemented by a cutback method using a TE mode source. The bending loss of the advanced bend with a radius of 25 μm is below 0.03 dB/90° in the C-band range. We summarized experimental results in Table III.

IV. DISCUSSIONS

A. SiN Photonics Integrated Circuit Routing Strategies

Fig. 3 shows the measured bending losses for a 50 μm radius circular bend, commonly used in SiN photonic integrated circuits. The bend losses are approximately 0.015–0.032 dB/90° at

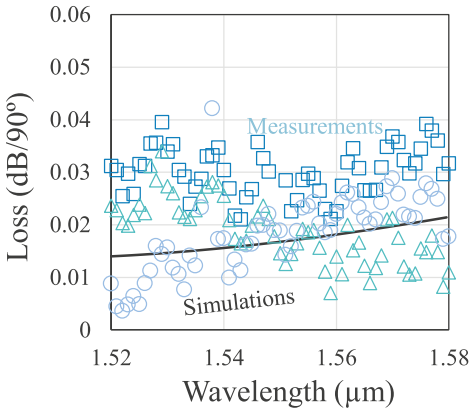

Fig. 3. Measurement results of circular bends with a 50 μm radius. Different shapes of polygons indicate different dies/wafers.

the wavelength of 1550 nm. Our measured results are consistent with the reported bending loss of 0.036 dB per 90° [6] for circular SiN bends. This range of losses is comparable to that of advanced bends with a 25 μm radius. Consequently, utilizing an advanced bend with a 25 μm radius instead of a 50 μm radius circular bend for waveguide routing in SiN photonic integrated circuits can significantly reduce the footprint.

B. Example SiN Ring Resonators Using Advanced Bends

The performance of SiN ring resonators with advanced bends is improved due to low round-trip losses resulting from reduced bending losses [11]. We fabricated ring resonators using these advanced bends, with each ring composed of four advanced bends. We used narrower bus waveguides than the 1μm-width single-mode waveguide, specifically a 0.55 μm waveguide. This narrower waveguide's mode has better phase matching with the concentric mode in the curved waveguide, leading to much weaker excitation of higher-order components [12]. Fig. 4 shows better symmetry of the field in the narrower straight waveguide. Fig. 4(c) presents an experimental comparison using different bus waveguides. In this experiment, the rings are circular, and the gap between the ring and bus is 0.57 μm.

Fig. 5 shows the ring resonators using advanced bends with a 15 μm radius. The quality (Q) factors, $\lambda/\Delta\lambda$ (where λ is the wavelength and $\Delta\lambda$ is the 3 dB bandwidth), of two ring resonators—one with circular bends and one with advanced bends—were compared. The Q-factor and the extinction ratio (ER) of the advanced ring resonator are higher than those of the normal ring resonator. The free spectral ranges (FSRs) were 12.9 nm and 12.4 nm for the circular and advanced bends, respectively. The ER is also an important characteristic of ring resonators. A higher ER enhances modulation depth, which improves the quality of the transmission signal (clear eye opening) when using ring resonators as micro ring modulators. The same conditions were used, including a narrowed bus waveguide of 0.55 μm and a gap of 0.57 μm.

Fig. 6 shows the highest Q-factor ring resonator from this fabrication run. The FSR was 7.4 nm and the Q-factor was 5.5 $\times$ 10^4. In this case, we used 25 μm radius advanced bends to

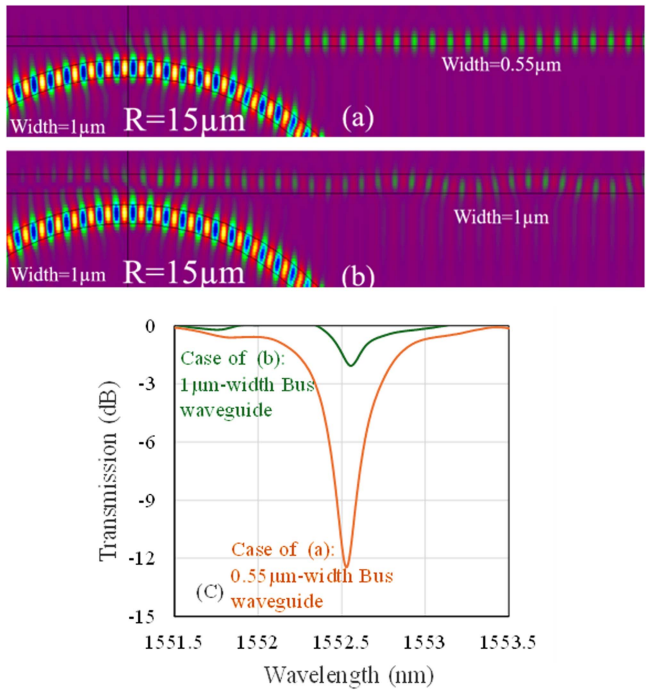

Fig. 4. (a) and (b) Electrical fields of ring and bus for coupling, and (c) measurement results of cases. All conditions are the same except the width of bus waveguides.

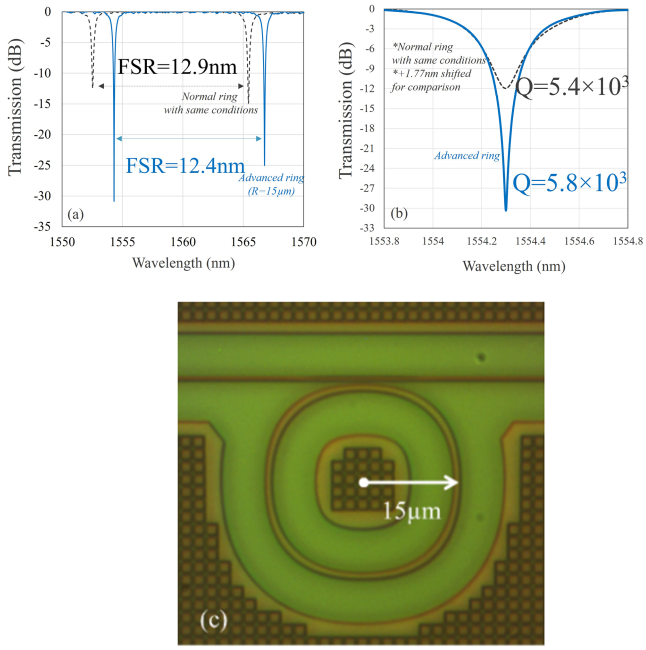

Fig. 5. (a) Measurement results of fabricated ring resonators, (b) Q-factor comparison, and (c) photo of ring resonator using advanced bends.

compose the ring and a narrowed bus waveguide of 0.55 μm. The gap between the ring and the bus was 0.50 μm.

Additionally, we simulated the influence of thickness variations, as shown in Fig. 7. The results indicate that for thickness variations up to 10 nm (from 400 nm to 390 nm), the change in the

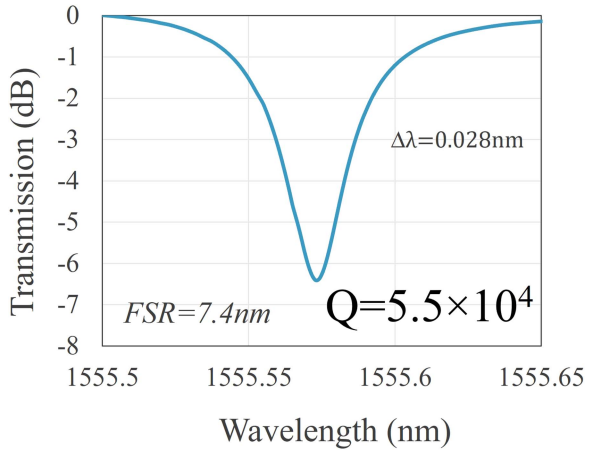

Fig. 6. The highest Q-factor among this wafer run. The ring resonator has advanced bends with a radius of 25 μm, narrowed bus waveguide of 0.55 μm and the gap of 500 nm.

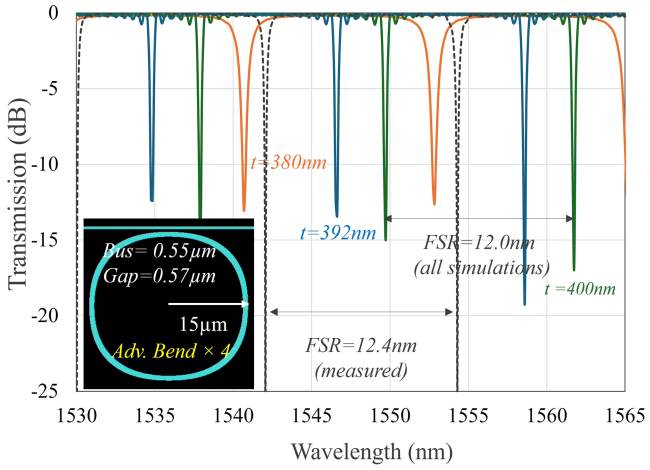

Fig. 7. Advanced ring resonator simulations were conducted to examine the effect of thicknesses of 400 nm(green), 392 nm(blue), and 380 nm(orange). The colored lines represent the simulations, while the dotted line indicates the measurement. The inset shows the simulation setup for 3D-FDTD.

Q factor is negligible. However, when the thickness is reduced to 380 nm, the Q factor significantly decreases. The thickness of the waveguide does not appear to influence the FSR.

V. Conclusion

Low-loss SiN bends were designed and experimentally demonstrated for the C-band. The bending losses of the advanced bends were nearly half those of circular bends with the same radii. Strategically, a 50 μm-radius circular bend can be replaced by a 25 μm-radius advanced bend, which has equivalent loss but reduced footprint. We also fabricated and measured micro ring resonators using advanced bends of silicon nitride waveguides. These achieved Q factors of 5.8×10^3 with a relatively large FSR of 12.4 nm and an ER of >30 dB when the radius was 15 μm. Additionally, the Q-factor was 5.5×10^4 when the radius was 25 μm.

References

[1] T. Kitoh, N. Takato, M. Yasu, and M. Kawachi, "Bending loss reduction in silica-based waveguides by using lateral offsets," *J. Lightw. Technol.*, vol. 13, no. 4, pp. 555–562, Apr. 1995.

[2] M. Cherchi, S. Ylinen, M. Harjanne, M. Kapulaninen, and T. Aalto, "Dramatic size reduction of waveguide bends on a micron-scale silicon photonic platform," *Opt. Exp.*, vol. 21, no. 15, pp. 17814–17823, 2013.

[3] J. H. Song, T. D. Kongnyuy, N. Hosseini, A. Stassen, R. Jansen, and X. Rottenberg, "Advanced waveguide bends for photonic integrated circuits," in *Proc. 45th Eur. Conf. Opt. Commun.*, 2019, pp. 1–3.

[4] J. H. Song, T. D. Kongnyuy, P. De Heyn, S. Lardenois, R. Jansen, and X. Rottenberg, "Low-loss waveguide bends by advanced shape for photonic integrated circuits," *J. Lightw. Technol.*, vol. 38, no. 12, pp. 3273–3279, Jun. 2020.

[5] J. H. Song, T. D. Kongnyuy, A. Stassen, V. Mukund, and X. Rottenberg, "Adiabatically bent waveguides on silicon nitride photonics for compact and dense footprints," *IEEE Photon. Technol. Lett.*, vol. 28, no. 20, pp. 2164–2167, Oct. 2016.

[6] F. Gao et al., "Low-loss and compact bends on multi-layer SiN-on-SOI platform for photonic integrated circuits," *IEEE Photon. Technol. Lett.*, vol. 33, no. 20, pp. 1131–1134, Oct. 2021.

[7] T. Sun and M. Xia, "Low loss modified Bezier bend waveguide," *Opt. Exp.*, vol. 30, pp. 10293–10305, 2022.

[8] F. Vogelbacher, S. Nevlacsil, M. Sagmeister, J. Kraft, K. Unterrainer, and R. Hainberger, "Analysis of silicon nitride partial Euler waveguide bends," *Opt. Exp.*, vol. 27, pp. 31394–31406, 2019.

[9] H. P. Bazargani, J. Flueckiger, L. Chrostowski, and J. Azaña, "Microring resonator design with improved quality factors using quarter Bezier curves," in *Proc. Conf. Lasers Electro-Opt.*, 2015, pp. 1–2, doi: 10.1364/CLEO_AT.2015.JTu5A.58.

[10] P. Helin, N. Pham, S. Lenci, A. R. Chaudhuri, A. Firrincieli, and M. Mannarino, "Silicon nitride photonic platform for sensing applications," in *Proc. Int. Conf. Opt. MEMS Nanophotonics*, 2019, pp. 38–39.

[11] J. H. Song, T. D. Kongnyuy, P. De Heyn, S. Lardenois, R. Jansen, and X. Rottenberg, "Enhanced silicon ring resonators using low-loss bends," *IEEE Photon. Technol. Lett.*, vol. 33, no. 6, pp. 313–316, Mar. 2021.

[12] Q. Xu, D. Fattal, and R. G. Beausoleil, "Silicon microring resonators with 1.5-μm radius," *Opt. Exp.*, vol. 16, pp. 4309–4315, 2008.